Laminar flow and heat transfer in a finned tube annulus

Ajay K. Agrawal
ME-EM Department, Michigan Technological University, Houghton, MI 49931, USA

Subrata Sengupta
Department of Mechanical Engineering, University of Miami, Coral Gables, FL 33124, USA

Laminar flow and heat transfer magnitudes in a finned tube annulus are obtained numerically. External circular fins on the inner tube are periodic. Pressure drop and heat transfer characteristics of the fins are obtained in the periodically fully developed region by varying geometric and flow parameters. Geometric parameters are annulus radius ratio (0.3 to 0.5), fin height/annular gap (0.33 to 0.67) and fin spacing/annular gap (2 to 5). Flow parameters are Reynolds number (100 to 1000) and Prandtl number (1 to 5). Comparisons are made with a plain tube annulus having the same length, heat transfer surface area, volume flow rate, and Reynolds number. The entire inter-fin space was found to be occupied by recirculating flow except at Reynolds numbers less than 500. A major contribution to heat transfer is made from the fin side at the downstream end. At Prandtl numbers less than 2, the use of fins may not be justified because the increase in pressure drop is more pronounced than the increase in heat transfer. At a Reynolds number of 1000 and a Prandtl number of 5, the heat transfer increases by a factor of 3.1, while the pressure drop increases by a factor of 2.3.

Keywords: augmentation and enhancement; finned surfaces; flow separation

Introduction

Development of high performance thermal systems—and the need for low capital and operating costs—have stimulated interest in methods to enhance heat transfer. Corrugations, fins, or extended surfaces are commonly used to increase heat transfer because they are relatively inexpensive and require no direct application of external power during operation.

Measurements of heat transfer and pressure drop in a parallel plate channel with triangular corrugations were made by O'Brien and Sparrow.[1] Heat transfer was found to increase by a factor of 2.5, with an increase in the pressure drop by an order of magnitude. Webb and Ramadhyani[2] studied laminar flow and heat transfer in a similar passage with straight fins. Fins blocking 25% of the flow with an aspect ratio (fin spacing/height) of 6 provided the best compromise between increases in heat transfer and pressure drop. At these values, heat transfer augmentation could be justified only for high Prandtl number (≥ 7) fluids. A similar study was done by Kelkar and Patankar[3] with conducting and nonconducting fins. The average Nusselt number due to highly conducting fins was 30–50% more than that due to nonconducting fins. At low Prandtl numbers, fins actually reduced heat transfer.

Flow and heat transfer in a tube with internal circumferential fins of height comparable to the tube diameter were studied by Rowley and Patankar.[4] Despite the increased surface area provided by fins, heat transfer could be reduced by flow diversion. Recirculating flow in the wake of the fins increased mixing, but the fins caused the main flow to move away from the heated wall. Consequently, total heat transfer decreased except at high Prandtl numbers.

For single-phase longitudinal flow over tubes, heat transfer augmentation by external roughness or low circular fins has been investigated in a number of studies.[5–8] In these studies, an externally enhanced tube was placed inside a circular tube, thereby forming an annulus. Pressure drop and heat transfer data were obtained for the flow in the annular region. Laminar flow and heat transfer in an annulus with a wavy inner tube were studied by Prata and Sparrow[9] and Agrawal and Sengupta.[10] Wavy inner tube was found to work best because it enhanced heat transfer with a relatively smaller increase in the pressure drop.

In this study, enhancement by external circular fins is investigated. An isothermally heated finned tube is placed inside an insulated circular tube. Pressure drop and heat transfer characteristics are obtained by varying fin height and spacing and the annular gap. Effects of the Reynolds number and the Prandtl number are studied for a geometry that yields optimum performance.

Formulation of the problem

An annulus with an externally finned inner tube is shown in Figure 1. Due to periodic change in the flow cross section caused by fins, the flow becomes periodically fully developed after an initial entrance region.[11] This work is limited to the periodically fully developed region. The flow is assumed to be laminar and steady, and viscous dissipation and buoyant forces are neglected. The fluid with constant properties is considered to be Newtonian and incompressible. The fins are assumed to be highly conducting.

Flow field

The velocity field is obtained from the solution of the Navier–Stokes equations expressed in the vorticity–stream function form. Dimensionless governing equations in axisymmetric

Address reprint requests to Dr. Agrawal at the ME-EM Department, Michigan Technological University, Houghton, MI 49931, USA.

Received 1 September; accepted 25 April 1989

cylindrical coordinates are:

Vorticity transport equation

$$\frac{\partial \Omega}{\partial t}+\frac{\partial}{\partial r}(u\Omega)+\frac{\partial}{\partial Z}(w\Omega)=\frac{1}{\mathrm{Re}}\left[\frac{\partial^2\Omega}{\partial r^2}+\frac{\partial^2\Omega}{\partial Z^2}+\frac{1}{r}\frac{\partial \Omega}{\partial r}-\frac{\Omega}{r^2}\right] \tag{1}$$

Vorticity definition equation

$$\frac{1}{r}\frac{\partial^2\psi}{\partial r^2}+\frac{1}{r}\frac{\partial^2\psi}{\partial Z^2}-\frac{1}{r^2}\frac{\partial \psi}{\partial r}=\Omega \tag{2}$$

Stream function definition equations

$$u=\frac{1}{r}\frac{\partial \psi}{\partial Z}; \qquad w=-\frac{1}{r}\frac{\partial \psi}{\partial r} \tag{3}$$

Nondimensional quantities in Equations 1–3 are defined as follows:

$$\psi=\psi^*/[w_m r_2^*]; \qquad \Omega=[\Omega^* r_2^*]/w_m;$$

$$t=[t^* w_m]/r_2^*; \qquad \mathrm{Re}=[w_m r_2^*]/\upsilon$$

where an asterisk (*) denotes a dimensional quantity.

Boundary conditions. At solid surfaces, no slip or impermeable conditions ($u=0$, $w=0$) are used. The stream function value at the outer wall is specified as zero ($\psi_o=0$). The stream function value at the inner wall and fins is obtained as

$$\psi_i=\frac{1-r_e^2}{2} \tag{4}$$

which corresponds to the volume flow rate in an annulus with a circular inner tube of radius, r_e. A circular tube of radius r_e provides the same surface area as the finned tube, i.e.,

$$r_e=\gamma+\frac{h^2+2\gamma h}{L_t} \tag{5}$$

Vorticity boundary conditions are obtained from Equation 2 using stream function boundary conditions. Due to the periodic nature of the flow, stream function and vorticity values at the inlet and the outlet are the same. Initial conditions are obtained from the solution of the fully developed flow in a circular tube annulus.

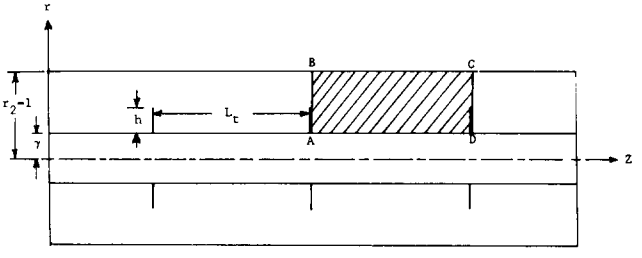

Figure 1 Geometric representation of the finned tube annulus

Pressure distribution

With $u=0$ and $w=0$, the axial momentum equation at the outer wall is

$$\left.\frac{dP}{dZ}\right|_o=\frac{1}{\mathrm{Re}}\left(\frac{\partial^2 w}{\partial r^2}+\frac{1}{r}\frac{\partial w}{\partial r}\right) \tag{6}$$

where pressure, P, has been nondimensionalized with respect to ρw_m^2. Pressure distribution along the outer wall is obtained by integrating Equation 6 in the axial direction. Pressure at the inlet is specified as zero.

Temperature field

The energy equation is

$$\frac{\partial T}{\partial t}+\frac{\partial}{\partial r}(uT)+\frac{\partial}{\partial Z}(wT)=\frac{1}{\mathrm{Pe}}\left(\frac{\partial^2 T}{\partial r^2}+\frac{\partial^2 T}{\partial Z^2}+\frac{1}{r}\frac{\partial T}{\partial r}\right)-\frac{uT}{r} \tag{7}$$

where temperature, T, has been nondimensionalized with respect to the wall temperature difference at the inlet.

Notation

A_s	Heat transfer surface area (Equation 11), m^2
D_h^*	Hydraulic diameter, $[2r_2^*(1-r_e)]$
EF	Enhancement factor, $[R_{\overline{Nu}}-1]/[R_{\Delta P}-1]$
G	Annular gap, $[1-\gamma]$
h	Fin height
$\bar{h}$	Average heat transfer coefficient (Equation 9), W/m^2 K
L_t	Fin spacing or cycle length
$\dot{m}$	Mass flow rate, kg/s
Nu	Local Nusselt number, $[-\partial T/\partial n\|_w]$
$\overline{Nu}$	Average Nusselt number in the finned tube annulus
Nu_a	Average Nusselt number in the circular tube annulus
n	Normal to the wall
P	Pressure, $[P^*/\rho w_m^2]$
ΔP	Total pressure drop in the finned tube annulus, $[P_{o2}-P_{o1}]$
ΔP_a	Total pressure drop in the circular tube annulus
Pe	Peclet number, [Re Pr]
Pr	Prandtl number
Q	Net heat transfer rate (Equation 10), W
Re	Reynolds number based upon r_2^*, $[w_m r_2^*/\upsilon]$
Re_D	Reynolds number based upon D_h^*, $[w_m D_h^*/\upsilon]$
$R_{\overline{Nu}}$	Average Nusselt number ratio, $\overline{Nu}/Nu_a$
$R_{\Delta P}$	Total pressure drop ratio, $[\Delta P/\Delta P_a]$
r	Radial coordinate
r_2^*	Outer tube radius, m
r_e	Radius of equivalent circular tube (Equation 5)
T	Temperature, $[T^*-T_{o1}^*]/[T_{i1}^*-T_{o1}^*]$
T_m	Mean temperature (Equation 13)
t	Time
u	Radial velocity
w	Axial velocity
w_m	Mean axial velocity, m/s
x_l	Length of the main recirculation eddy
Z	Axial coordinate
γ	Radius ratio
Ω	Vorticity
ψ	Stream function
ψ_l	Strength of the main recirculation eddy, $[(\psi_{max}-\psi_i)/\psi_i]$

Subscripts and superscripts

1	Inlet
2	Outlet
i	Inner wall
o	Outer wall
w	Wall
*	Dimensional quantity

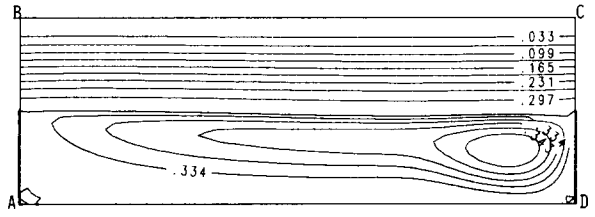

Figure 2a Streamline pattern: $Re_D = 1000$, $G = 0.6$, $h = 0.3$, $L_t = 1.8$, Time = 0 ($x_t = 1.8$, $\psi_o = 0.33$, $\psi_t = 7.8\%$)

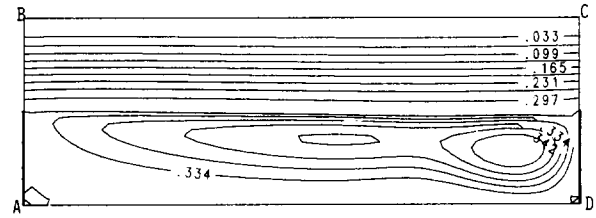

Figure 2b Streamline pattern: $Re_D = 1000$, $G = 0.6$, $h = 0.3$, $L_t = 1.8$, Time = 0.75 ($x_t = 1.8$, $\psi_o = 0.33$, $\psi_t = 7.4\%$)

Boundary conditions. The inner wall surface, including the fins, is kept at a constant temperature (i.e., fins are assumed to be highly conducting). The outer wall is insulated ($\partial T/\partial n|_o = 0$). Temperature boundary conditions at the inlet and the outlet are obtained by a procedure similar to that used by Kelkar and Patankar[3] for periodically fully developed flows. Initial conditions are obtained from the solution of the fully developed heat transfer in a circular tube annulus.

Nusselt number definitions. The local Nusselt number corresponds to the local heat flux ($Nu = -\partial T/\partial n|_w$). The average Nusselt number is defined as

$$\overline{Nu} = \frac{\bar{h} D_h^*}{k} \tag{8}$$

where the overall heat transfer coefficient, $\bar{h}$, is obtained from the overall heat balance.

$$\bar{h} = \frac{Q}{A_s \Delta T_m} \tag{9}$$

Quantities appearing in Equation 9 are the net heat transfer rate, Q, the heat transfer surface area, A_s, and the mean temperature difference, ΔT_m, given as

$$Q = \dot{m} c_p (T_{m2} - T_{m1}) \tag{10}$$

$$A_s = 2\pi r_e^* L_t^* \tag{11}$$

$$\Delta T_m = \frac{(T_w - T_{m1}) + (T_w - T_{m2})}{2} \tag{12}$$

where T_{m1} and T_{m2} are bulk temperatures at the inlet and the outlet, respectively. The bulk temperature T_m is defined as

$$T_m = \frac{r_1^1 \int Twr\, dr}{r_1^1 \int wr\, dr} \tag{13}$$

Solution procedure

Computations are performed in the symmetry region A–B–C–D shown in Figure 1. Equations 1 and 7 are integrated over the control volume to obtain finite-difference forms of vorticity transport and energy equations. Finite differencing is done, using the power-law scheme suggested by Patankar.[12] Central differencing is used for derivatives in the remaining equations. Steady state solutions for the flow field and temperature distribution are obtained by marching in time. At each time step, coupled vorticity and stream function equations are solved by an iterative procedure. Iterations are required to obtain correct vorticity boundary conditions, particularly at the start of the solution. The vorticity equation is solved, using the alternate direction implicit (ADI) method. The stream function equation is solved, using Gauss–Seidel iteration. Once the vorticity steady state is achieved, the energy equation is solved, using the ADI method. Steady state is confirmed when the change in the total pressure drop (ΔP) and the average Nusselt number ($\overline{Nu}$) in 500 time steps is within 1%.

The mathematical model and the computer program were verified using analytical solutions for the circular tube annulus. These results and various tests for grid size convergence were presented in Refs. 10, 13, and 14. Present computations were made from a grid having 31 radial and 73 axial points.

Results and discussion

Base condition

To facilitate direct comparison, flow and heat transfer with fins are obtained at the base conditions investigated by Agrawal and Sengupta.[10] These conditions are: $Re_D = 1000$, $Pr = 1$, $\gamma = 0.4$ (or $G = 0.6$), $h = 0.3$, and $L_t = 1.8$.

Flow field. The streamline pattern in the annular domain is shown in Figure 2. Due to the sudden change in cross section, the flow separates at the tip of the fin. The entire region between fins is occupied by recirculating flow. Immediately past the fin, the flow is nearly stagnant. Higher velocities exist toward the downstream end, where the recirculation eddy is centered. Flow in the separated region was found to be periodically oscillating, with a period of oscillation of about 3.5. Most of the time the flow pattern is as shown in Figure 2a. However, at time $t = 0.75$, two eddies are present in the recirculating region, as shown in Figure 2b. In both cases, mass flow in the major eddy (ψ_t) is about 8% of that in the main flow. Influence of fins on the main flow is small. Attached flow is similar to that in a circular tube annulus of radius ratio ($\gamma + h$).

Pressure distribution at the outer wall for finned and circular tube annuli is shown in Figure 3. Note that the fins cause an increase in the total pressure drop. Pressure gradient is high

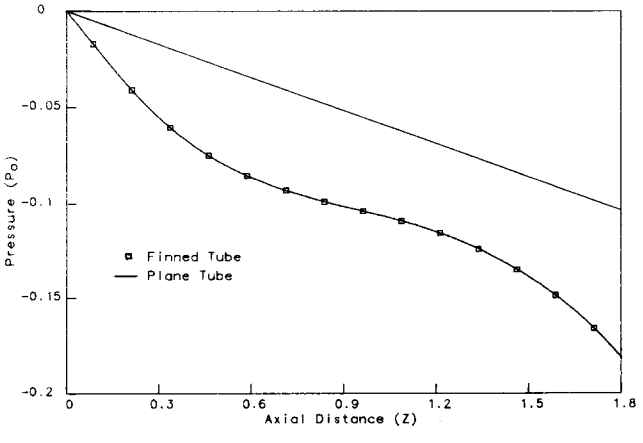

Figure 3 Pressure along the outer wall: $Re_D = 1000$, $G = 0.6$, $h = 0.3$, $L_t = 1.8$

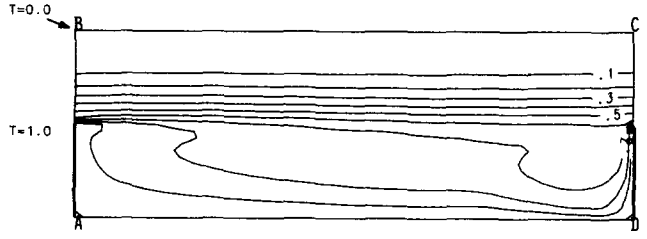

Figure 4 Isotherms: $Re_D = 1000$, $G = 0.6$, $h = 0.3$, $L_t = 1.8$

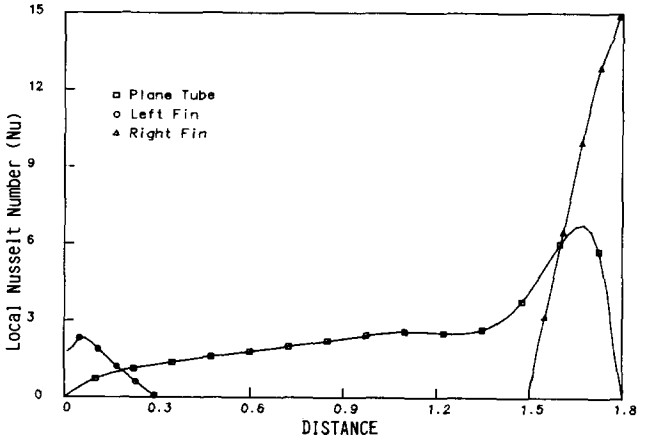

Figure 5 Local Nusselt number: $Re_D = 1000$, $G = 0.6$, $h = 0.3$, $L_t = 1.8$

near the fins, but in the middle region the pressure gradient is relatively small. Circular fins do not assist in pressure recovery at the outer wall because the recirculation region has little effort on the main flow.

Temperature field. The flow field shown in Figure 2a persists about 80% of the time, so it is used to obtain the temperature distribution. Figure 4 shows isotherms in the finned tube annulus. In the upstream end of the inter-fin space (close to the left fin), spacing between isotherms is large, indicating a region of low temperature gradients. This condition is caused by an almost stagnant flow in this region, which restricts heat transfer to diffusion only. In the downstream end, close to the right fin, the isotherms are closely spaced.

Local Nusselt numbers at the fins and along the circular tube are shown in Figure 5. From the left (upstream) fin, heat transfer is higher at the tip and decreases to zero at the base. Heat flux from the inner tube increases in the downstream direction until a peak value, which occurs near the center of the recirculation eddy, is reached. Thereafter the heat flux decreases until the base of the right fin is reached, where it is zero. Heat transfer in the downstream region is high due to increased convection aided by higher velocities in the recirculation eddy. Maximum heat transfer occurs at the tip of the right (downstream) fin where the main flow reattaches. It can be inferred from Figure 5 that heat transfer from the downstream end of the fin is several times higher than that from the upstream end.

Overall performance. Fins cause the total pressure drop and the average Nusselt number to increase. For the case discussed above, the pressure drop increases by 81% (or $R_{\Delta P} = 1.81$), while the heat transfer increases by only 18% ($R_{\overline{Nu}} = 1.18$), resulting in an enhancement factor ($EF = [R_{\overline{Nu}} - 1]/[R_{\Delta P} - 1]$) of 0.22. In contrast, a wavy tube of Gaussian shape studied by Agrawal and Sengupta[10] resulted in an enhancement factor close to 1.

Effect of geometric parameters

Fin height. As shown in Figure 6, both the total pressure drop and the average Nusselt number increase with fin height. At $h = 0.2$, although the pressure drop increases by about 35%, heat transfer remains the same. The reason is that the decrease in heat transfer in the upstream region is not compensated for by an increase near the center of the eddy. At $h = 0.4$, the average Nusselt number increases by about 50%. However, due to large flow blockage, the pressure drop increases by a factor of nearly 3.

Annular gap. Annular gap has little effect on the pressure drop ratio and the Nusselt number ratio, as shown in Figure 7. Both decrease slightly as the annular gap decreases. The Nusselt number ratio decreases because a larger fraction of flow area is occupied by the separated region. It should be noted that these ratios are obtained by using the pressure drop and the Nusselt number values in a circular tube annulus, both of which increase as the annular gap decreases.

Fin spacing. Pressure drop and heat transfer increase with fin spacing (or cycle length), as shown in Figure 8. Closely spaced fins actually decrease heat transfer. Thus fin performance improves if the fins are farther apart. At $L_t = 3.0$, the maximum

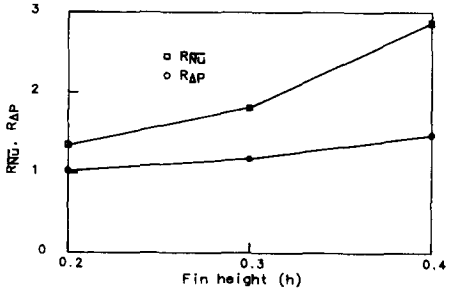

Figure 6 Effect of fin height: $Re_D = 1000$, $Pr = 1.0$, $G = 0.6$, $L_t = 1.8$

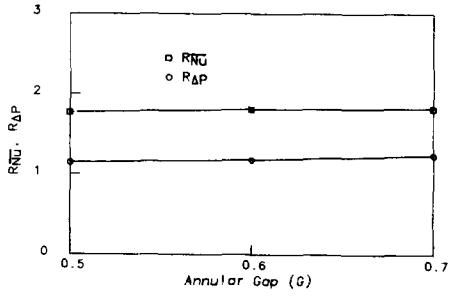

Figure 7 Effect of annular gap: $Re_D = 1000$, $Pr = 1.0$, $h = 0.3$, $L_t = 1.8$

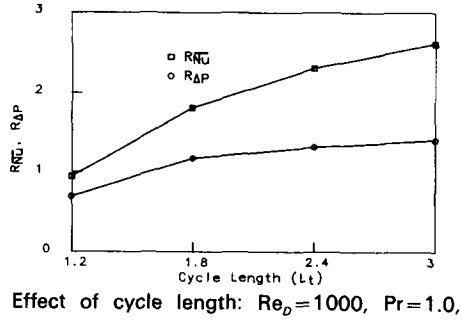

Figure 8 Effect of cycle length: $Re_D = 1000$, $Pr = 1.0$, $G = 0.6$, $h = 0.3$

Table 1 Effect of geometric parameters on performance characteristics of the finned tube annulus

Purpose	Re_D	Pr	h	G	L_t	r_e	$R_{\Delta P}$	$R_{\overline{Nu}}$	EF
Base case	1000	1.0	0.3	0.6	1.8	0.583	1.81	1.18	0.22
Effect of fin height	1000	1.0	0.2	0.6	1.8	0.511	1.34	1.02	0.06
			0.3			0.583	1.81	1.18	0.22
			0.4			0.667	2.86	1.47	0.25
Effect of annular gap	1000	1.0	0.3	0.5	1.8	0.717	1.77	1.15	0.19
				0.6		0.583	1.81	1.18	0.22
				0.7		0.400	1.82	1.24	0.29
Effect of cycle length	1000	1.0	0.3	0.6	1.2	0.675	0.94	0.69	*
					1.8	0.583	1.81	1.18	0.22
					2.4	0.538	2.30	1.32	0.25
					3.0	0.510	2.61	1.41	0.25
Optimum geometric parameters	1000	1.0	0.3	0.7	3.0	0.390	2.29	1.39	0.30

* No heat transfer enhancement

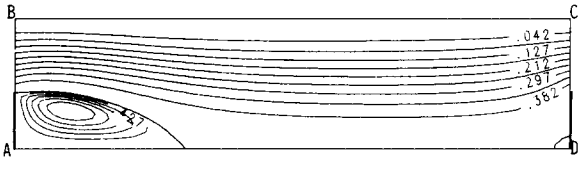

Figure 9a Streamline pattern: $Re_D=100$, $G=0.7$, $h=0.3$, $L_t=3.0$ ($x_f=0.55$, $\psi_o=0.424$, $\psi_f=4.3\%$)

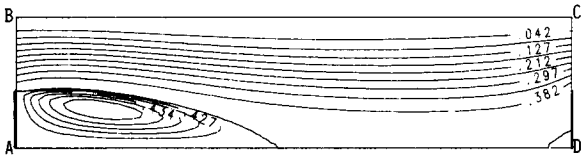

Figure 9b Streamline pattern: $Re_D=200$, $G=0.7$, $h=0.3$, $L_t=3.0$ ($x_f=0.85$, $\psi_o=0.424$, $\psi_f=4.8\%$)

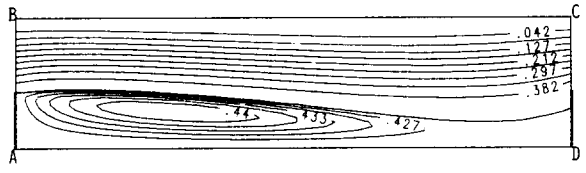

Figure 9c Streamline pattern: $Re_D=500$, $G=0.7$, $h=0.3$, $L_t=3.0$ ($x_f=3.00$, $\psi_o=0.424$, $\psi_f=4.5\%$)

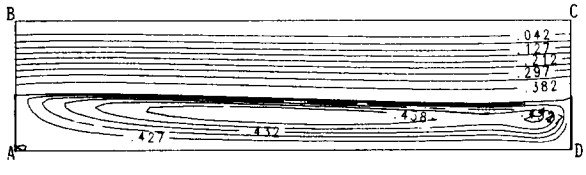

Figure 9d Streamline pattern: $Re_D=1000$, $G=0.7$, $h=0.3$, $L_t=3.0$ ($x_f=3.00$, $\psi_o=0.424$, $\psi_f=4.0\%$)

fin spacing studied, $R_{\overline{Nu}}=1.41$, $R_{\Delta P}=2.61$, and hence EF = 0.25 are obtained.

Optimum geometric parameters. Performance characteristics of the finned tube annulus are given in Table 1. As discussed earlier, increased fin spacing and annular gap result in better performance of the finned tube annulus. From these observations, optimum geometric parameters were obtained at base-flow conditions: $\gamma=0.3$ (or $G=0.7$), $h=0.3$, and $L_t=3.0$.

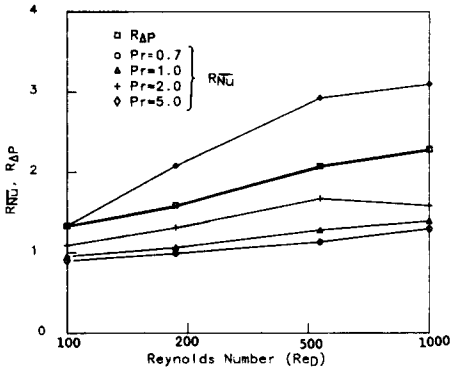

Figure 10 Effect of flow parameters: $G=0.7$, $h=0.3$, $L_t=3.0$

Effects of flow parameters

Effects of flow parameters were studied for the optimum geometric parameters. Streamline patterns for four different Reynolds numbers are shown in Figure 9. At low Reynolds numbers, the flow separates at the tip of the fin, but reattaches at the inner tube wall. Only part of the inter-fin space is occupied by the recirculation eddy, which is centered in the wake of the left fin. Streamline curvature, evident at Re = 500, disappears at higher Reynolds numbers (= 1000) since the flow reattaches near the tip of the right fin.

Effects of the Reynolds number and the Prandtl number on the performance of fins are shown in Figure 10. These results are also summarized in Table 2. At all Reynolds numbers, the fins cause an increase in the overall pressure drop. Heat transfer increases only if $Re_D Pr \geq 200$. Use of fins may not be justified at low Prandtl numbers because the increase in the pressure drop is much higher than the increase in heat transfer. However, fins are effective if $Pr \geq 5$.

Conclusions

The entire inter-fin space is occupied by recirculating flow except at Reynolds numbers of less than 500. The attached flow is similar to that in a circular tube annulus. The pressure gradient is high near the fins, but the separated region near the inner wall does not promote pressure recovery at the outer wall. The major contribution to the total heat transfer is from the fin side at the downstream end. From the inner tube, heat transfer is low except in the downstream region, where the recirculation eddy is centered. Heat transfer from the fin side at the upstream end is rather small.

Table 2 Effect of geometric parameters on performance of the finned tube annulus

Purpose	Re_D	Pr	h	G	L_t	r_e	$R_{\Delta P}$	$R_{\overline{Nu}}$	EF
Effect of Reynolds number	100	1.0	0.3	0.7	3.0	0.39	1.33	0.95	*
	200						1.59	1.07	0.12
	500						2.08	1.28	0.26
	1000						2.29	1.39	0.30
Effect of Prandtl number	100	0.7	0.3	0.7	3.0	0.39	1.33	0.90	*
		1.0					1.33	0.95	*
		2.0					1.33	1.09	0.27
		5.0					1.33	1.33	1.00
	200	0.7	0.3	0.7	3.0	0.39	1.59	0.99	*
		1.0					1.59	1.07	0.12
		2.0					1.59	1.31	0.53
		5.0					1.59	2.08	1.83
	500	0.7	0.3	0.7	3.0	0.39	2.08	1.13	0.12
		1.0					2.08	1.28	0.26
		2.0					2.08	1.67	0.62
		5.0					2.08	2.93	1.79
	1000	0.7	0.3	0.7	3.0	0.39	2.29	1.30	0.23
		1.0					2.29	1.39	0.30
		2.0					2.29	1.58	0.45
		5.0					2.29	3.10	1.63

* No heat transfer enhancement

The increase in the pressure drop is more pronounced than the increase in heat transfer, especially at low Prandtl numbers. The enhancement factor (EF) of a finned tube annulus is only $\frac{1}{4}$ the enhancement factor of a wavy tube annulus. Fins effectively enhance heat transfer only at high Prandtl numbers. For example, at a Reynolds number of 1000 and a Prandtl number of 5, heat transfer increases by a factor of 3.1, while the pressure drop increases by a factor of 2.3.

References

1 O'Brien, J. E. and Sparrow, E. M. Corrugated-duct heat transfer, pressure drop, and flow visualization. *ASME J. Heat Transf.* 1982, **104**, 410–416

2 Webb, B. W. and Ramadhyani, S. Conjugate heat transfer in a channel with staggered ribs. *Int. J. Heat and Mass Transf.* 1985, **28**, 1679–1687

3 Kelkar, K. M. and Patankar, S. V. Numerical prediction of flow and heat transfer in a parallel plate channel with staggered fins. *ASME J. Heat Transf.* 1987, **109**, 25–30

4 Rowley, G. J. and Patankar, S. V. Analysis of laminar flow and heat transfer in tubes with internal circumferential fins. *Int. J. Heat and Mass Transf.* 1984, **27**, 553–560

5 Dalle Donne, M. and Meyer, L. Turbulent convective heat transfer from rough surfaces with two-dimensional rectangular ribs. *Int. J. Heat and Mass Transf.* 1978, **20**, 583–620

6 Obermeier, E. and Schaber, A. Experimental investigation of heat transfer from transverse finned tubes with longitudinal flow. *Proceedings of the Sixth International Heat Transfer Conference.* Hemisphere, Washington, D.C., 1978

7 Geiger, G. E. and Mandal, S. K. Heat transfer and friction factors of high Prandtl number laminar flow through an annulus with circumferential fins. *Proceedings of the Sixth International Heat Transfer Conference.* Hemisphere, Washington, D.C., 1978

8 Hsieh, S. S. Thermal characteristics of annular flow with asymmetrically roughened surfaces. *Int. J. Heat and Fluid Flow.* 1988, **9**, 78–82

9 Prata, A. T. and Sparrow, E. M. Heat transfer and fluid flow characteristics for an annulus of periodically varying cross-section. *Numer. Heat Transf.* 1984, **7**, 285–304

10 Agrawal, A. K. and Sengupta, S. Pressure drop and heat transfer in annuli with periodic enhancements on tube side: Effects of geometric and flow parameters. *Proceedings of the Symposium on Fundamentals of Forced Convection Heat Transfer.* ASME HTD-Vol. 101, 1988

11 Berner, C., Durst, F., and McEligot, D. M. Flow around baffles. *ASME J. Heat Transf.* 1984, **106**, 743–749

12 Patankar, S. V. *Numerical Heat Transfer and Fluid Flow.* Hemisphere, Washington, D.C., 1980

13 Agrawal, A. K. and Sengupta, S. Fluid flow and heat transfer through blocked annuli. *Numer. Heat Transf.*, 1989

14 Agrawal, A. K. and Sengupta, S. Recirculating flow and heat transfer in an axisymmetric cavity bounded by a cylinder. *Convective Transport*, eds. Y. Jaluria *et al.*, ASME HTD-Vol. 82, 1–7, 1987